

Synchrotron Strain Measurements for *in situ* Formed Metallic Glass Matrix Composites

R.T. Ott¹, F. Sansoz², J.F. Molinari², J. Almer³, C. Fan¹, and T.C. Hufnagel¹

¹Department of Materials Science and Engineering, Johns Hopkins University, Baltimore, MD 21209

²Department of Mechanical Engineering, Johns Hopkins University, Baltimore, MD 21209

³Argonne National Laboratory, Advanced Photon Source, Argonne, IL 60439

ABSTRACT

We have examined the micromechanical behavior of *in situ* formed metallic glass composites by performing *in situ* high-energy synchrotron X-ray scattering during uniaxial compression. The load partitioning between the amorphous matrix and the reinforcing particles was examined by measuring the lattice strains in the crystalline particles during compressive loading. The crystalline particles yield in compression during loading followed by tensile yielding during unloading. The large elastic mismatch between the two phases leads to large residual strains after each loading cycle. The load partitioning was also examined with finite element modeling (FEM). The predicted von Mises effective stress in the crystalline particles from the FEM calculations compares well with the experimentally determined von Mises effective stress so long as the deformation is elastic in both particles and matrix. After the particles yield, the model predicts strain hardening of the particles that is not observed experimentally.

INTRODUCTION

In situ formed metallic glass composites are amorphous metallic alloys in which a crystalline second phase is precipitated during processing [1-4]. Unlike typical metal matrix composites (MMCs), metallic glass matrix composites consist of a macroscopically brittle matrix reinforced with a ductile crystalline phase that is stiffer than the surrounding glass matrix. Therefore, during loading the crystalline reinforcing phase yields first via dislocation motion, followed by yielding in the stronger glass matrix by shear band formation. The ductile crystalline second phase particles act as barriers to shear band propagation in addition to being preferential sites for shear band formation. The combination of these two processes leads to an increase in plastic strain prior to failure exhibited by the composite alloys compared to monolithic metallic glasses. The heterogeneous initiation of shear bands at the particle/matrix interface is the result of stress concentrations that develop between the crystalline phase and the amorphous matrix due to the elastic mismatch. The elastic mismatch also affects the load partitioning between the two phases.

The applied stress at which the crystalline particles yield at is a function of the load transfer between the matrix and the particles. Previous studies have used high-energy X-ray scattering to measure the load partitioning among phases in MMCs[5-7]. More recently, high-energy X-ray scattering has been used for *in situ* strain measurements in metallic glass matrix composites produced *ex situ* (that is, by adding crystalline particles to the molten alloy prior to casting)[8].

In this work, we report on *in situ* strain measurements using high-energy X-ray scattering on *in situ* formed metallic glass matrix composites. The composite alloys consist of Ta-rich particles dispersed in an amorphous matrix. The measured load partitioning between the two phases is compared with finite element modeling (FEM) predictions.

EXPERIMENTAL AND NUMERICAL APPROACH

Composite alloys of composition $(\text{Zr}_{70}\text{Cu}_{20}\text{Ni}_{10})_{90-x}\text{Ta}_x\text{Al}_{10}$ ($x = \text{at. \% Ta}$) were prepared by arc melting in a two step process which is described in detail elsewhere^[3,9]. The samples were suction cast into a copper mold to form rods 3.2 mm in diameter. The composition of the crystalline particles was measured by wavelength dispersive spectroscopy to be approximately $\text{Ta}_{93}\text{Zr}_5(\text{Al} + \text{Cu} + \text{Ni})_2$. The volume percentage of the Ta-rich particles in the composites was approximately 4%, as determined by quantitative optical microscopy and scanning-electron microscopy. The compression samples were machined to 2.50 mm in diameter and 5 mm in length, and the ends of the samples were polished to ensure parallelism.

The *in situ* strain measurements were performed at the 1-ID beamline of the Advanced Photon Source at Argonne National Laboratory. The samples were loaded in compression from 0 to 1750 MPa in steps of 10 – 100 MPa using a screw driven load cell. Monochromatic 80.7 keV (0.0154 nm) X-rays were used to measure the lattice strains for each load. A digital image plate (MAR 345) with a 150 x 150 μm pixel size was positioned 975 mm downstream from the sample to record the Debye rings from the Ta-rich particles. The lattice strains present in the Ta-rich particles during loading were calculated using a data analysis procedure similar to that used by Wanner and Dunand^[6].

A 2D plane-strain computational model for a metallic glass matrix composite was built using the finite element method (FEM). In this model, the composite is viewed as a microstructure with two phases (Ta-rich particles embedded within an amorphous matrix), which are treated with separate constitutive laws. Particular attention was paid to capture the exact morphology and dimensions of the composite structure. For that purpose, a mesh-generating program, ppm2oof^[10], was used with micrographs of the material taken by scanning electron microscopy. A discrete model of the image was obtained and, subsequently refined, near all the boundaries between the two phases using ppm2oof.

The calculations were conducted by assigning a series of compressive load increments in the top section of the mesh and by constraining the bottom nodes in the direction of loading. A symmetry plane was enforced on the left side of the mesh by fixing the displacement of nodes in a direction perpendicular to the loading axis. The resolution scheme is based on a Lagrangian framework using an explicit time integration algorithm. Further details on the implementation of this method, but in the context of 2D axisymmetric, can be found elsewhere^[11]. The maximum applied load corresponds to a uniform pressure of 1800 MPa. The load was applied proportionally to the loading time, which was set to a relatively large value so that quasi-static loading conditions are simulated. In the present case, this value represents 10^{-5} s.

RESULTS AND DISCUSSION

The applied stress vs. lattice strain for the Ta-rich particles measured from the BCC-Ta $\{2\ 1\ 1\}$ reflection during a loading-unloading cycle is shown in Figure 1. The strains in the longitudinal (parallel to loading axis) and transverse (normal to loading axis) directions are shown. The lattice strains are not zero at an applied load of 0 MPa due to thermal residual strains that develop during processing. The thermal strains, which are hydrostatic in nature, were calculated using the Eshelby equivalent inclusion method^[12] and simply added to the measured lattice strains.

For applied stresses below 300 MPa, the measured lattice strain is linear which indicates elastic loading in the crystalline particles. Above 300 MPa however, the lattice strain deviates from linearity, consistent with particle yielding. This results in a decrease in the amount of load transferred to the Ta-rich particles. As the composite alloy is loaded above 300 MPa, the Ta-rich particles flow plastically while the glass matrix remains elastic. However, at an applied stress of ~1450 MPa, the lattice strain displays another marked change in its slope for the both the longitudinal and transverse directions. The change in the slope indicates an increase in the load being transferred to the Ta-rich particles.

Upon unloading the Ta-rich particles undergo a reversal in their strain state. The large elastic strain that is stored in the amorphous matrix is released as the applied stress is removed. The particles deform elastically in tension down to an applied stress of approximately 600 MPa (compressive). For applied stresses below 600 MPa there is an inflection in the curve indicating that the particles have yielded in tension. When the applied stress is completely removed, the particles are left with a very large residual tensile strain in the longitudinal direction and compressive strain in the transverse direction.

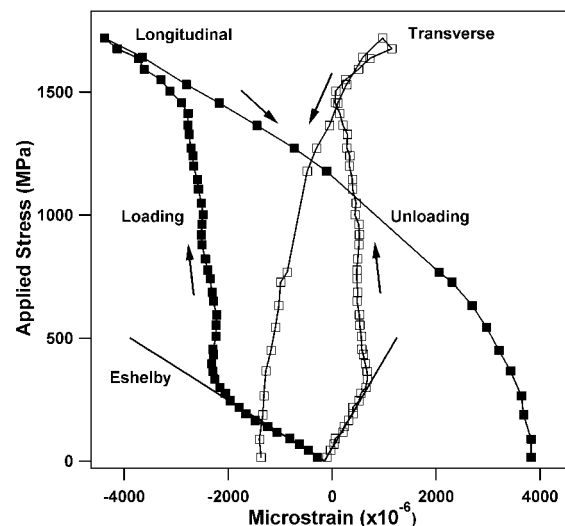


Figure 1. Measured $\{2\ 1\ 1\}$ lattice strain for Ta-rich particles during uniaxial compression. The predicted elastic strain using the Eshelby equivalent inclusion method is also shown. Loading and unloading are indicated by the upward and downward arrows respectively.

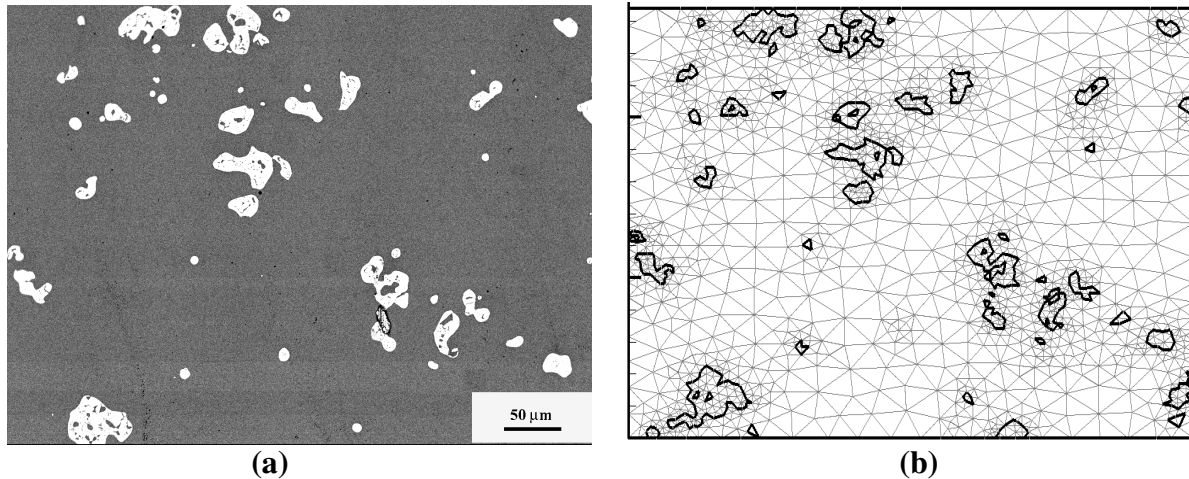


Figure 2. (a)SEM micrograph representative of 8% Ta containing alloy along with (b) the mesh generated from the micrograph for the FEM calculations.

To further examine the micromechanics of the composite alloy we used FEM to calculate the load partitioning that occurs during uniaxial compressive loading. Figure 2(b) shows the mesh that was used to perform the calculations. The mesh contains approximately 3200 6-node triangular elements. The mesh is representative of the 8% Ta alloy which contains ~ 4% Ta-rich particles. Figure 3 shows the von Mises effective stress calculated from the experimentally measured lattice strains along with the results from the FEM calculation. For the Ta-rich particles, the constitutive properties of pure Ta were used in the FEM calculation^[13]. However, since the particles are actually a Ta-rich solid solution (as described above), it is likely that the constitutive properties for pure Ta do not fully describe the behavior of the Ta-rich particles. In particular, we expect that the yield strength of the particles is greater than that of pure Ta with an equivalent grain size. To partially account for this, we performed uniaxial compression tests (not shown) on samples of Ta-rich solid solution alloys of similar composition to the particles. The results indicate that the yield stress for the particles is 335 ± 55 MPa. We also expect differences in the strain hardening behavior of the alloys and pure Ta. However, to date we have not been able to obtain reliable data on strain hardening of the alloys, so the strain hardening behavior of pure Ta was used for all of the simulations (the amorphous matrix was assumed to be elastic-perfectly plastic with no work hardening). The FEM results using different yield strengths for the Ta-rich particles are shown in Figure 3.

The experimental data (Fig. 3) show that the Ta-rich particles yield at a von Mises stress of approximately 400 MPa. After yielding, the von Mises stress remains essentially constant with no apparent work hardening. While this behavior is the subject of ongoing investigation, it may be due to the change in the nature of the matrix constraint during plastic flow (because the Ta particles become essentially incompressible with $\nu=0.5$ after yield) or due to a yield-drop phenomenon associated with Lüders band formation (as is seen in other BCC alloys).

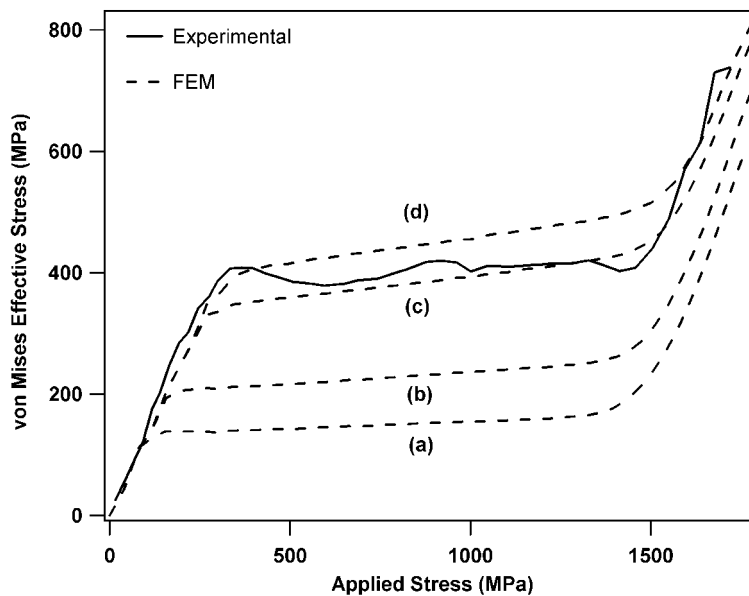


Figure 3. Von Mises effective stress for the particles calculated from experimental data and from FEM. The yield strength of the Ta-rich particles in the FEM calculations is assumed to be (a) 120 MPa, (b) 180 MPa, (c) 300 MPa, and (d) 350 MPa. The amorphous matrix was assumed to have a yield strength of 1750 MPa and $\nu = 0.38$.

The FEM results show a strong dependence on the assumed yield stress of the particles (discussed above). When the yield strength of the Ta-rich particles is assumed to be 120 MPa (corresponding to that of pure Ta) the calculated von Mises curve does not agree with the experimental data (Fig. 3). Good agreement, however, can be achieved by assuming a yield strength of 350 MPa, which agrees with the experimentally measured yield strength of the Ta solid-solution alloys.

For all of the FEM calculations, the magnitude of the predicted work hardening in the Ta-rich particles is greater than what is experimentally observed; this is the subject of ongoing investigation. However, all of the models accurately predict the behavior of the crystalline particles at high applied stresses (> 1450 MPa). Similar to the experimental data, the FEM results indicate a large increase in the load being carried by the Ta-rich particles at applied stresses above 1450 MPa. The increase in the load transfer to the particles is the result of yielding in the surrounding amorphous matrix. The increase in the load being partitioned to the particles results in the large increase in the von Mises stress as shown in Figure 3. However, the increase in load transfer does not result in work hardening in the composite alloy.

CONCLUSIONS

The *in situ* strain measurements show that the Ta-rich particles undergo three different loading regimes. For low applied stresses, the deformation is linearly elastic. For higher applied stress, the particles experience plastic flow, which results in a decrease in the load transferred to the

particles. There is no apparent strain hardening of the particles through this range. For large applied stresses, matrix yielding results in a significant increase in the amount of load transferred to the crystalline particles. FEM calculations accurately capture the elastic behavior and the yield stress, if it is taken into account that the particles have a higher yield stress than pure Ta. The calculations, however, predict greater work hardening behavior than which we experimentally observed. This is probably because the strain-hardening behavior of the particles is different from that of pure Ta (the strain-hardening exponent of which was used for the calculations).

ACKNOWLEDGEMENTS

The authors thank D. Dunand and M. Young (Northwestern) for their comments and assistance with the *in situ* strain measurements. We gratefully acknowledge support for this work from several sources: R. T. Ott from the National Science Foundation (NSF) under grant DMR-9875115; T. C. Hufnagel from NSF under grant DMR-0307009; F. Sansoz, J. F. Molinari and C. Fan from the Army Research Laboratory (ARL) under grant DAAD-190120003. Use of the Advanced Photon Source was supported by the U. S. Department of Energy, Office of Science, Office of Basic Energy Sciences, under Contract No. W-31-109-Eng-38. The views expressed are those of the authors, and not necessarily those of NSF, ARL, or DOE

- ¹C.C. Hays, C.P. Kim, and W.L. Johnson, *Phys.Rev. Lett.* **84**, 2901 (2000).
- ²U. Kuhn, J. Eckert, N. Mattern, and L. Schultz, *Appl. Phys. Lett.* **80** (14), 2478 (2002).
- ³C. Fan, R.T. Ott, and T.C. Hufnagel, *App. Phys. Lett.* **81**, 1020 (2002).
- ⁴H. Ma, J. Hu, and E. Ma, *App. Phys. Lett.* **83**, 1020 (2003).
- ⁵M.R. Daymond, and P.J. Withers, *Scripta Mater.* **35**, 1229 (1996).
- ⁶A. Wanner and D.C. Dunand, *Metall. Mater. Trans. A* **31A**, 2949 (2000).
- ⁷E. Maire, A. Owen, and J.Y. Buffiere, *Acta Mater.* **49**, 153 (2001).
- ⁸D.K. Balch, E. Üstündag , and D.C. Dunand, *J. Non-Cryst. Solids* **317**, 176 (2003).
- ⁹R.T. Ott, C. Fan, J. Li, and T.C. Hufnagel, *J. Non-Cryst. Solids* **317**, 158 (2003).
- ¹⁰ppm2oof, *software*, <http://www.ctcms.nist.gov/oof>.
- ¹¹J.F. Molinari, *Finite Elements in Analysis and Design* **38**, 921 (2002).
- ¹²T.W. Clyne and P.J. Withers, *An Introduction to Metal Matrix Composites* (Cambridge University Press, Cambridge, 1993).
- ¹³A.S. Khan and R. Liang, *Int. J. of Plasticity* **15**, 1089 (1999).